

Supporting Information

for

Stereoselectivity in Oxyallyl–Furan 4+3 Cycloadditions: Control of Intermediate Conformations and Dispersive Stabilisation in Cycloadditions involving Oxazolidinone Auxiliaries

Elizabeth H. Krenske, K. N. Houk,* Andrew G. Lohse, Jennifer E. Antoline, and Richard P. Hsung*

Department of Chemistry and Biochemistry, University of California, Los Angeles, CA 90095, and Division of Pharmaceutical Sciences and Department of Chemistry, University of Wisconsin, Madison, WI 53705

Part 2 – Experimental Data

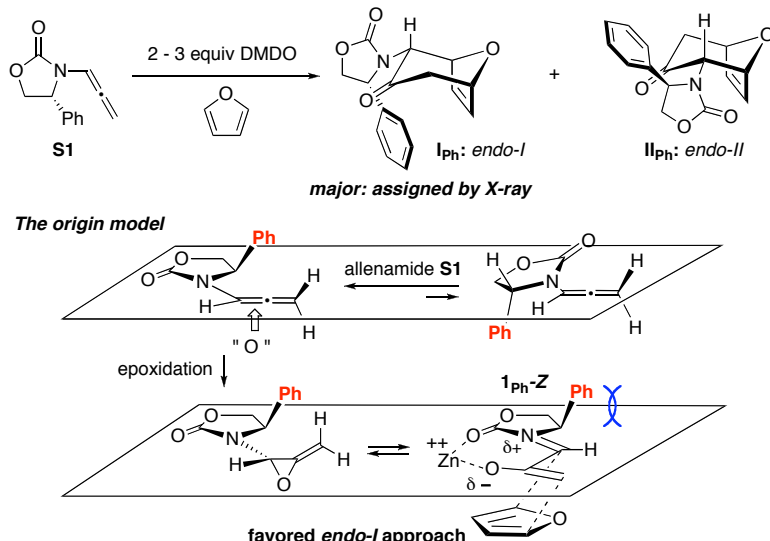
REASSIGNMENT AND CONFIRMATION OF STEREOCHEMICAL OUTCOME

IN INTERMOLECULAR [4 + 3] CYCLOADDITIONS OF FURAN WITH

N-STABILIZED OXYALLYL CATIONS DERIVED FROM DMDO-EPOXIDATIONS OF CHIRAL ALLENAMIDES

In 2001, Hsung¹ reported a diastereoselective [4 + 3] cycloaddition of furan with *N*-stabilized chiral oxyallyl cations generated from epoxidation of oxazolidinone-substituted allenamides **S1** [Scheme S1]. The originally proposed model was based on the *Z*-oxyallyl cation **1_{Ph}-Z** being the operative intermediate for the cycloaddition, especially in the presence of Zn cation, and that steric presence of the Ph substituent on the Evans' oxazolidinone auxiliary would favor the approaching furan from the bottom face of the π -manifold in **1_{Ph}-Z**, leading to the stereochemically confirmed [via X-ray] *endo*-*I* **I_{Ph}** as the major isomer. Consequently, all other cycloaddition examples were assigned based on a direct correlation with this model [Table S1].

Scheme S1



at -78 °C without ZnCl₂: 70% yield; *endo*-*I* : *endo*-*II* [I_{Ph} : II_{Ph}] = 82 : 18
at -78 °C with 2.0 equiv ZnCl₂: 80% yield; *endo*-*I* : *endo*-*II* [I_{Ph} : II_{Ph}] ≥ 94 : 6

Table S1 [See Reference-1]

entry	allenamide	additive ^a	cycloadduct	yields ^b	<i>endo</i> <i>I</i> : <i>II</i> ^c	entry	allenamide	additive ^a	cycloadduct	yields ^b	<i>endo</i> <i>I</i> : <i>II</i> ^c
1		ZnCl ₂		40%	≥ 95 : 5	5		None		74%	≥ 95 : 5
2		ZnCl ₂		60%	≥ 95 : 5	6		None		62%	93 : 7
3		ZnCl ₂		83%	≥ 96 : 4	7		None		70%	55 : 45
4		None		67%	77 : 23	8		None		72%	94 : 6

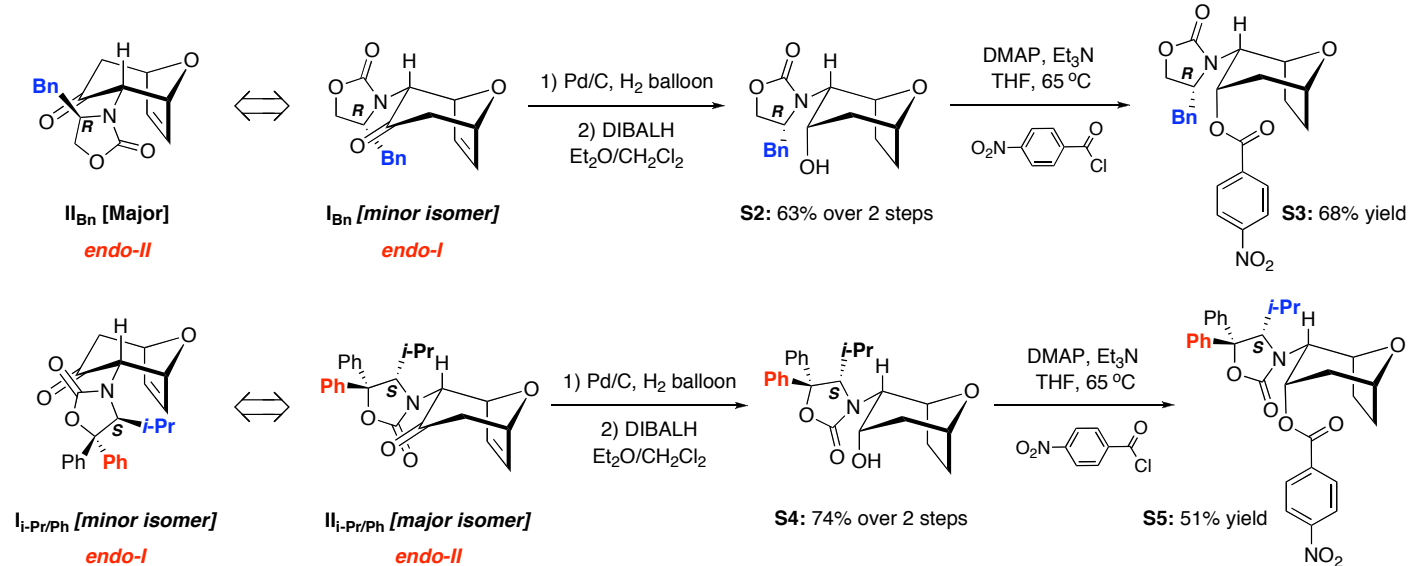
a) All reactions were carried out in THF at -40 to -50 °C in the presence of 2.0-3.0 equiv of DMDO [as a solution in acetone] and 10.0 equiv of the diene. All reactions were completed within 8 h. b) All yields are isolated yields. c) Only the *endo* diastereoisomers were observed in these reactions. Ratios were determined by using ¹H and/or ¹³C NMR.

Reference 1: Xiong, H., Hsung, R. P., Berry, C. R., Rameshkumar, C. *J. Am. Chem. Soc.* 2001, 123, 7174-7175.

However, Houk's DFT calculations suggesting that the *E*-oxyallyl cation was the lowest energy conformer led to a very different mechanistic model. If the cycloaddition proceeds through the *E*-oxyallyl cation, then instead of being controlled by steric repulsion between furan and the Ph group on the oxazolidinone auxiliary, "steric attraction" or CH- π interaction between furan and Ph would dictate the stereochemical outcome of the cycloaddition with furan selectively approaching from the more hindered face of the π -manifold in the *E*-oxyallyl cation [see **Figure S1** on next page].

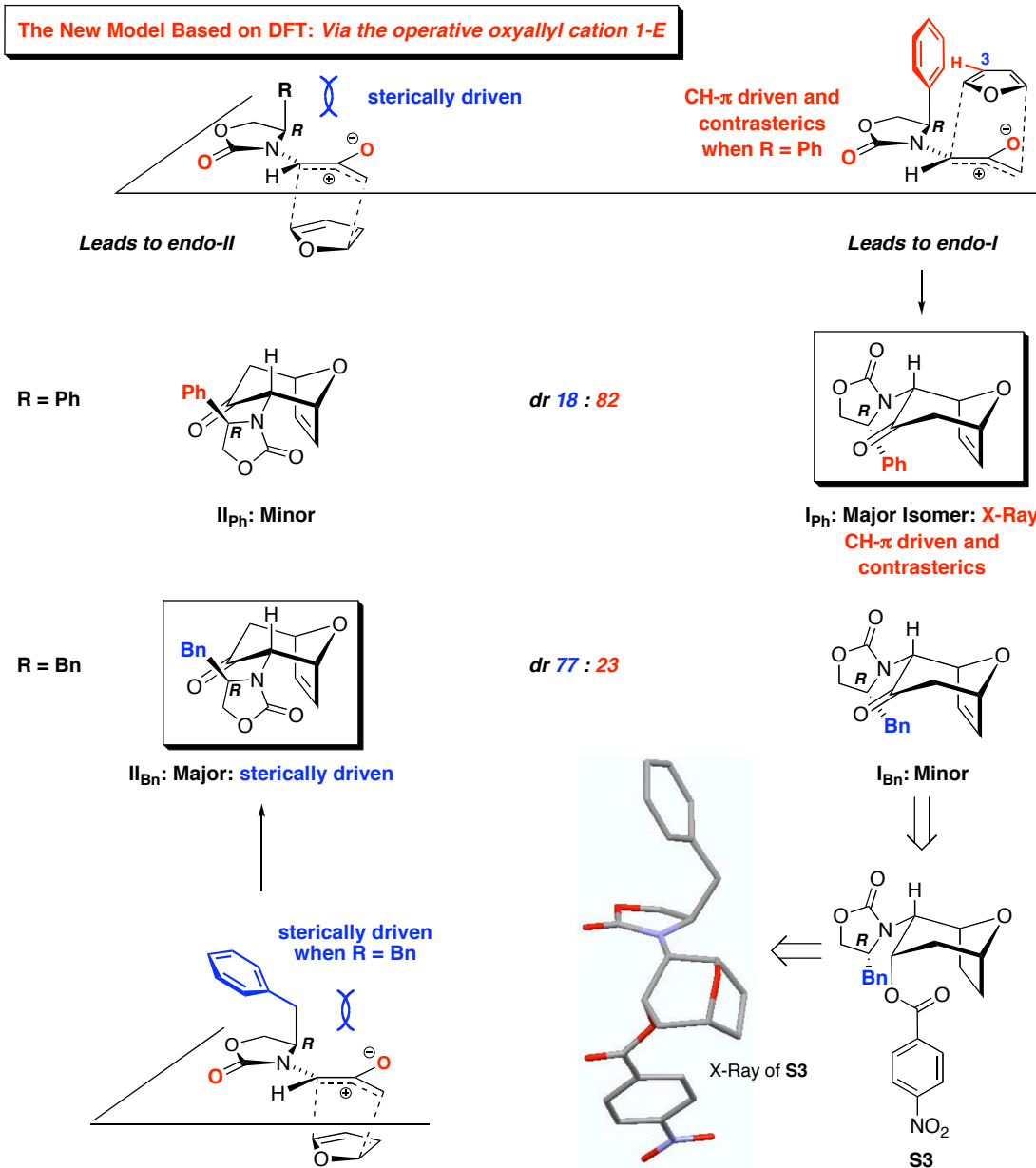
This new finding prompted a reevaluation of stereochemical determinations for other cycloadducts especially the two examples in entries 4 and 8 because they constitute two other substitution patterns on the oxazolidinone-based auxiliaries that differ from the Ph-substituted oxazolidinone auxiliary [**Table S1**]. Consequently, we pursued relevant X-ray structures. Reduction of the carbonyl in both cycloadducts **I**_{Bn} [**the minor isomer**] and **II**_{i-Pr/Ph} [**the major isomer**] followed by conversion of the respective alcohols **S2** and **S4** led to the *para*-nitrobenzoate esters **S3** and **S5**, which afforded X-ray quality crystals [**Scheme S2**].

Scheme S2



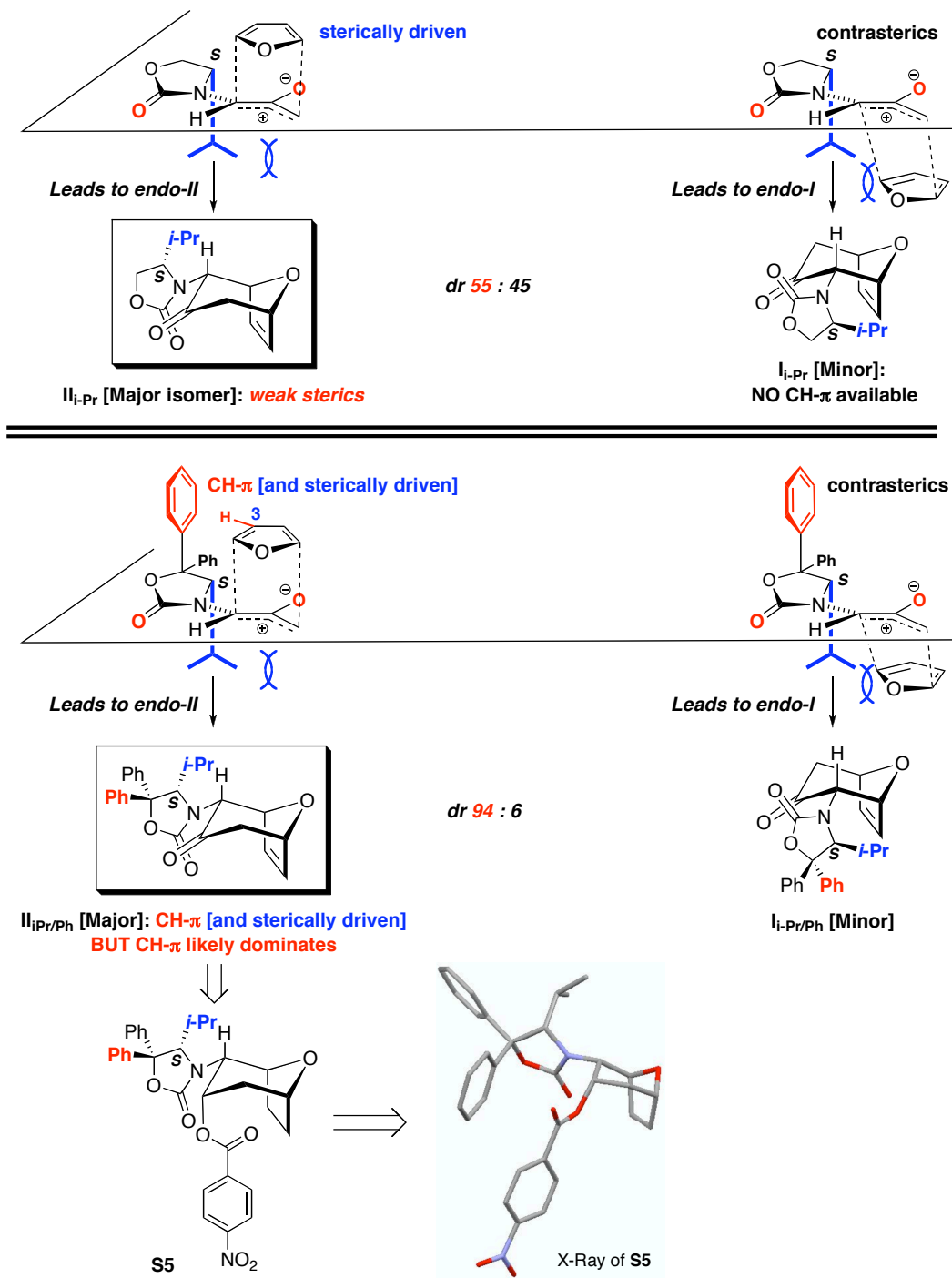
X-Ray structures of both *para*-nitrobenzoate esters **S3** and **S5** were acquired and revealed that their stereoselectivities were opposite from that which had originally been supposed. Based on the new mechanistic model, replacement of the Ph substituent on the oxazolidinone with a Bn group eliminates the possibility of stabilizing CH- π interaction. Consequently, the new model would predict that *endo-II* be the major isomer from the cycloaddition driven by pure steric repulsion when using Evans' Bn-substituted oxazolidinone auxiliary. X-Ray structure of **S3** confirms the prediction that *endo-II* [**II**_{Bn}] was indeed the major cycloadduct with **I**_{Bn} [**minor**] now being concisely assigned as *endo-I* [**Figure S1**]. This represents a complete reversal of diastereoselectivity from that of the Ph-substituted oxazolidinone auxiliary.

Figure S1



On the other hand, while Evans' $^{\text{t}}\text{Pr}$ -substituted oxazolidinone auxiliary led to a poor diastereoselectivity [see II_{ipr} versus I_{ipr} in Figure S2], adopting Seebach's 4(*S*)- $^{\text{t}}\text{Pr}$ -5,5-di-Ph-oxazolidinone auxiliary gave a very high *dr* in the [4 + 3] cycloaddition [see $\text{II}_{\text{ipr/Ph}}$]. This result had always been puzzling to us. Based on the original steric repulsion model through the Z-oxyallyl cation, the only explanation we offered was “additional steric presence of the geminal diphenyl groups” likely pushed the $^{\text{t}}\text{Pr}$ group closer toward the cycloaddition manifold in the transition state, thereby rendering a greater steric presence than simply using Evans’ $^{\text{t}}\text{Pr}$ -substituted oxazolidinone auxiliary.

Figure S2



However, the new model presents a much better clarification, as X-ray data of **S5** supports the theoretical prediction that the endo-*II* cycloadduct would be the major isomer through a CH- π interaction between furan and the Ph group at the 5-position *trans* to i-Pr [Figure S2]. While the steric factor cannot be completely ruled out, given the distinct contrast between these two sets of oxazolidinone auxiliaries, we believe the CH- π interaction plays a much greater role in the stereochemical control.

GENERAL EXPERIMENTAL INFORMATION

All reactions were performed in flame-dried glassware under nitrogen atmosphere. Solvents were distilled prior to use. Reagents were used as purchased from Aldrich, Acros, Alfa Aesar, or TCI) unless otherwise noted. Chromatographic separations were performed using Silicycle 43-60 Å SiO₂. ¹H and ¹³C NMR spectra were obtained on Varian VI-400 and VI-500 spectrometers using CDCl₃ with TMS or residual solvent as standard unless otherwise noted. Melting points were determined using a Laboratory Devices MEL-TEMP and are uncorrected/calibrated. Infrared spectra were obtained on Bruker EQUINOX 55 FTIR. TLC analysis was performed using Aldrich 254 nm polyester-backed plates (60 Å, 250 µm) and visualized using UV and KMnO₄ stains. Low-resolution mass spectra were obtained using an Agilent 1100 series LS/MSD and are APCI. High-resolution mass spectral analysis performed at University of Wisconsin School of Pharmacy and Department of Chemistry Mass Spectrometry Laboratories. All spectral data obtained for new compounds are reported here.

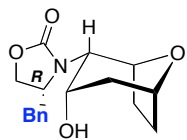
PREPARATIONS OF NITRO-ESTERS FOR X-RAY STRUCTURAL ANALYSIS

Hydrogenation/ Dibal-H Reduction. To a solution of the cycloadduct (0.10 mmol) in EtOAc (4 mL) at rt was added 5% Pd/C (~5-10 mg). The heterogeneous mixture was stirred under 1 atm H₂ for 4 h. Filtration through CeliteTM led to the desired hydrogenated product that was carried on to the next step without further purification.

To a stirring solution of the above crude hydrogenated product in Et₂O/CH₂Cl₂ (3 mL: 2:1 ratio) at -78 °C was added DIBAL-H (0.25 mL, 1.0 M in toluene). The reaction was stirred for 1 h before warming to rt over 1 h. The reaction was quenched with sat aq NH₄Cl, and the aqueous layer was separated and extracted with Et₂O (3 x 25 mL). The combined organic extracts were washed with sat aq NaCl, dried over Na₂SO₄, filtered, and concentrated *in vacuo*. The crude residue was purified via silica gel flash column chromatography (isocratic eluent: EtOAc in hexanes) affording the desired alcohol [S2 or S4].

Esterification. To a solution of the alcohol prepared above (0.05 mmol) in THF (0.5 mL) at rt were added DMAP (0.60 mg, 0.0050 mmol), Et₃N (13.7 µL), and 4-nitrobenzoyl chloride (14.0 mg, 0.075 mmol). The reaction was stirred overnight at 65 °C and monitored by TLC. Upon completion, the solution was concentrated *in vacuo* and the crude residue was purified via silica gel flash column chromatography (isocratic eluent: EtOAc in hexanes) affording the desired nitro-ester [S3 or S5].

CHARACTERIZATIONS



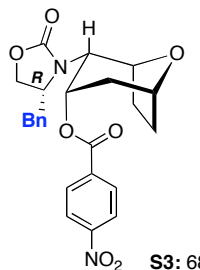
S2: 63% over 2 steps

S2: R_f = 0.13 [1:1 EtOAc/hexanes]; colorless oil;

^1H NMR (500 MHz, CDCl_3) δ 1.88 (d, 1H, J = 14.5 Hz), 1.95-2.01 (m, 2H), 2.11 (dt, 1H, J = 4.0, 14.5 Hz), 2.39-2.43 (m, 1H), 2.68-2.71 (m, 1H), 2.72 (dd, 1H, J = 6.0, 13.5 Hz), 3.16 (dd, 1H, J = 4.0, 14.0 Hz), 3.69 (t, 1H, J = 3.5 Hz), 4.09-4.14 (m, 1H), 4.18 (dd, 2H, J = 8.0, 16.5 Hz), 4.26 (brs, 1H), 4.43 (brs, 2H), 4.60 (brs, 1H), 7.18 (d, 2H, J = 7.0 Hz), 7.28 (t, 1H, J = 7.5 Hz), 7.34 (t, 2H, J = 7.0 Hz);

^{13}C NMR (125 MHz, CDCl_3) δ 26.8, 29.1, 38.3, 38.4, 57.7, 58.6, 66.9, 67.1, 74.9, 127.6, 129.2, 129.3, 129.4, 135.3, 159.0;

mass spectrum (APCI): m/e (% relative intensity) 304 (100) ($\text{M}+\text{H}$) $^+$, 286 (75).



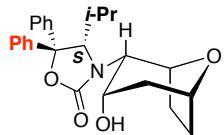
S3: 68% yield

S3: R_f = 0.30 [1:1 EtOAc/hexanes]; yellow crystals; mp 222-223 °C; $[\alpha]_D^{23} = 16.2$ [c 0.85, CHCl_3];

^1H NMR (400 MHz, CDCl_3) δ 1.98 (d, 1H, J = 15.6 Hz), 2.14-2.24 (m, 2H), 2.29-2.41 (m, 2H), 2.73 (dd, 1H, J = 10.8, 13.6 Hz), 2.85 (ddd, 1H, J = 4.8, 8.8, 12.8 Hz), 3.10 (dd, 1H, J = 2.8, 12.8 Hz), 3.84 (tt, 1H, J = 1.6, 8.8 Hz), 3.97-4.02 (m, 2H), 4.35 (t, 1H, J = 3.6 Hz), 4.53 (dd, 1H, J = 4.4, 6.4 Hz), 4.68 (dd, 1H, J = 3.2, 7.6 Hz), 5.88 (t, 1H, J = 4.4 Hz), 7.13 (d, 2H, J = 6.8 Hz), 7.28 (d, 1H, J = 7.2 Hz), 7.33 (t, 2H, J = 6.8 Hz), 8.18 (d, 2H, J = 9.2 Hz), 8.32 (d, 2H, J = 8.8 Hz);

^{13}C NMR (125 MHz, CDCl_3) δ 27.4, 29.3, 36.0, 39.6, 55.9, 57.1, 66.6, 71.5, 74.1, 75.1, 124.1, 127.7, 129.1, 129.3, 130.6, 135.4, 135.5, 150.9, 157.5, 164.1;

mass spectrum (APCI): m/e (% relative intensity) 453 (50) ($\text{M}+\text{H}$) $^+$, 286 (100).



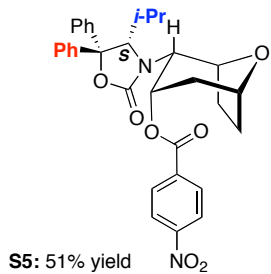
S4: 74% over 2 steps

S4: $R_f = 0.29$ [1:1 EtOAc/hexanes]; white solid; mp 289-290 °C;

^1H NMR (500 MHz, CDCl_3) δ 0.86 (d, 3H, $J = 7.0$ Hz), 1.09 (d, 3H, $J = 7.0$ Hz), 1.80-1.83 (m, 1H), 1.94-1.99 (m, 3H), 2.06 (sept, 1H, $J = 7.0$ Hz), 2.34-2.38 (m, 1H), 3.64 (t, 1H, $J = 3.0$ Hz), 4.04 (brs, 1H), 4.28-4.32 (m, 2H), 5.10 (d, 1H, $J = 4.0$ Hz), 7.23-7.26 (m, 1H), 7.31-7.35 (m, 3H), 7.42 (t, 2H, $J = 8.0$ Hz), 7.50 (d, 2H, $J = 7.5$ Hz), 7.72 (d, 2H, $J = 8.0$ Hz);

^{13}C NMR (125 MHz, CDCl_3) δ 16.0, 22.3, 28.0, 28.8, 30.0, 37.2, 60.6, 65.3, 69.0, 74.4, 75.2, 87.8, 124.6, 125.9, 127.9, 128.6, 128.9, 129.4, 138.3, 144.5, 156.2;

mass spectrum (APCI): m/e (% relative intensity) 408 (100) $(\text{M}+\text{H})^+$.



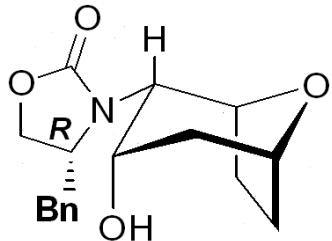
S5: 51% yield

S5: $R_f = 0.42$ [1:1 EtOAc/hexanes]; white solid; mp 330-332 °C; $[\alpha]_D^{23} = -40.8$ [c 0.70, CHCl_3];

^1H NMR (400 MHz, CDCl_3) *Exists as a mixture of rotational isomers in ~4:1 ratio:* major isomer: δ 0.86 (d, 3H, $J = 6.8$ Hz), 1.14 (d, 3H, $J = 7.2$ Hz), 1.65 (ddd, 1H, $J = 4.0, 9.6, 12.8$ Hz), 1.90 (d, 1H, $J = 15.2$ Hz), 1.93-2.00 (m, 2H), 2.18 (dt, 1H, $J = 4.0, 15.6$ Hz), 2.27 (tdd, 1H, $J = 4.4, 7.6, 12.8$ Hz), 3.05 (ddd, 1H, $J = 4.4, 9.6, 14.0$ Hz), 3.92 (t, 1H, $J = 3.6$ Hz), 4.29 (d, 1H, $J = 1.6$ Hz), 4.36 (dd, 1H, $J = 4.0, 7.2$ Hz), 5.14 (dd, 1H, $J = 2.8, 7.2$ Hz), 5.24 (brs, 1H), 6.58 (t, 1H, $J = 7.2$ Hz), 6.79 (t, 2H, $J = 7.2$ Hz), 7.18 (t, 1H, $J = 7.2$ Hz), 7.25 (t, 2H, $J = 8.0$ Hz), 7.36 (d, 3H, $J = 8.0$ Hz), 7.82 (d, 2H, $J = 8.8$ Hz), 8.18 (d, 2H, $J = 9.2$ Hz); partial resonances for minor isomer: δ 1.07 (d, 3H, $J = 7.2$ Hz), 1.40 (t, 2H, $J = 7.2$ Hz), 3.18-3.24 (m, 2H), 3.54-3.60 (m, 2H), 4.04 (t, 1H, $J = 4.0$ Hz), 4.31 (d, 1H, $J = 1.6$ Hz), 7.54 (d, 2H, $J = 9.2$ Hz), 8.27 (d, 2H, $J = 8.8$ Hz);

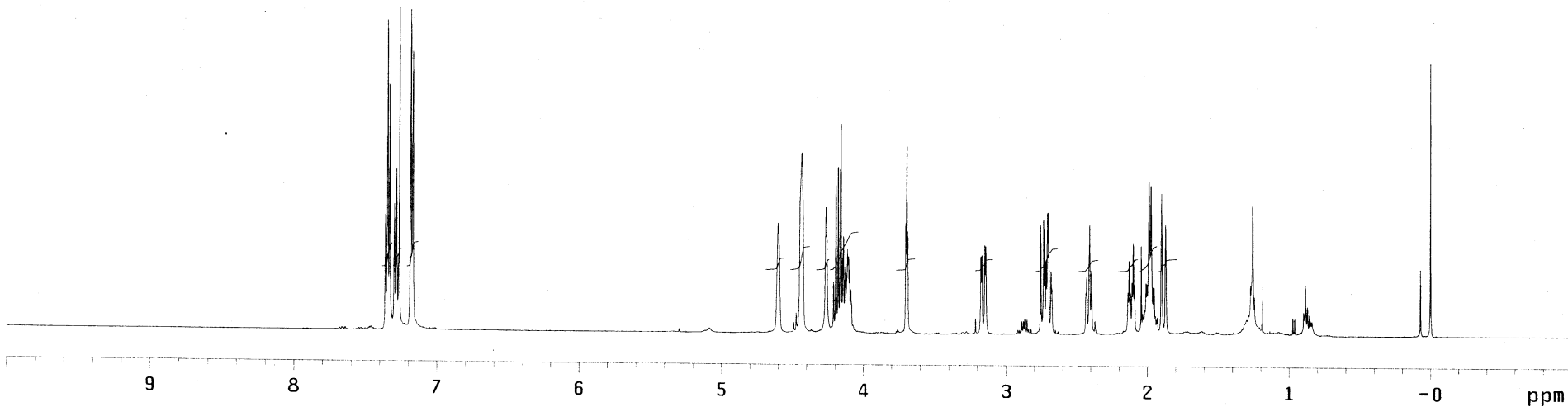
^{13}C NMR (100 MHz, CDCl_3) δ 15.8, 22.7, 28.6, 29.1, 30.1, 35.8, 59.3, 68.6, 69.1, 74.0, 76.0, 87.5, 123.5, 124.1, 125.9, 127.6, 127.7, 128.4, 128.6, 130.9, 134.9, 138.8, 144.4, 150.6, 155.7, 164.1;

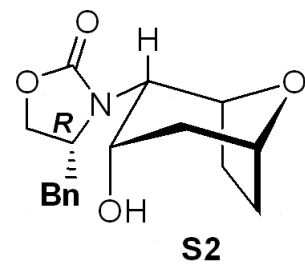
mass spectrum (APCI): m/e (% relative intensity) 557 (100) $(\text{M}+\text{H})^+$.



S2

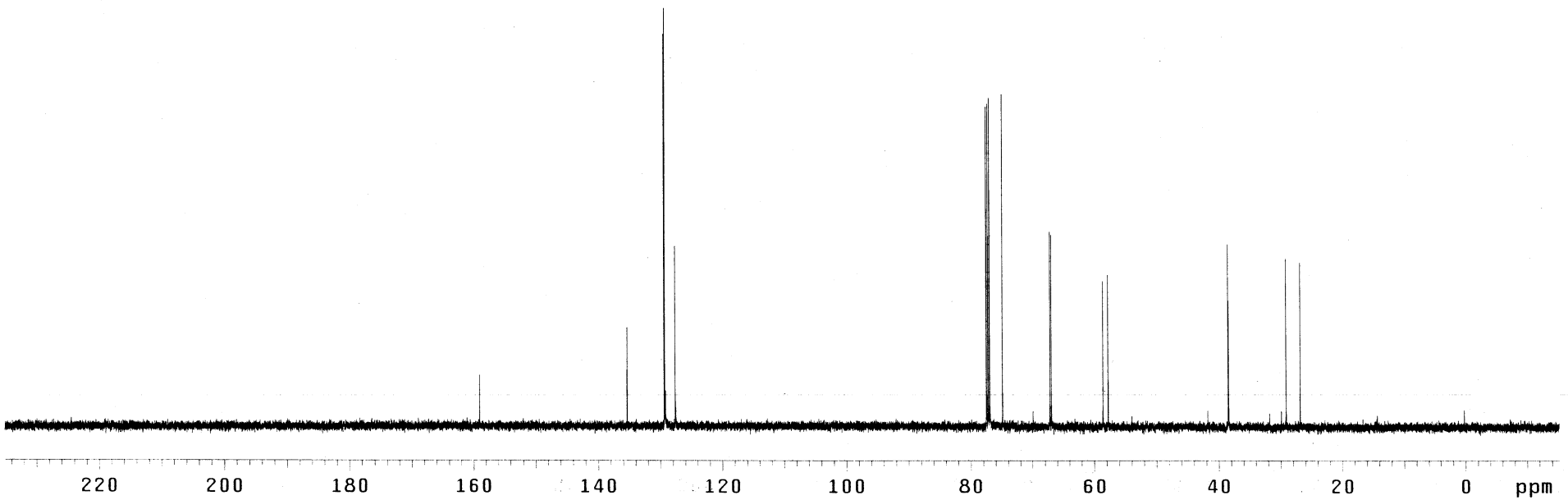
500 MHz, CDCl_3

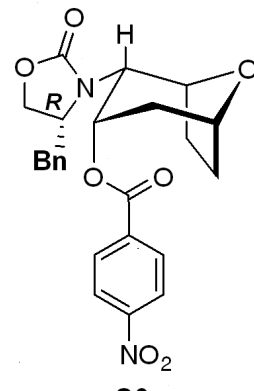




S2

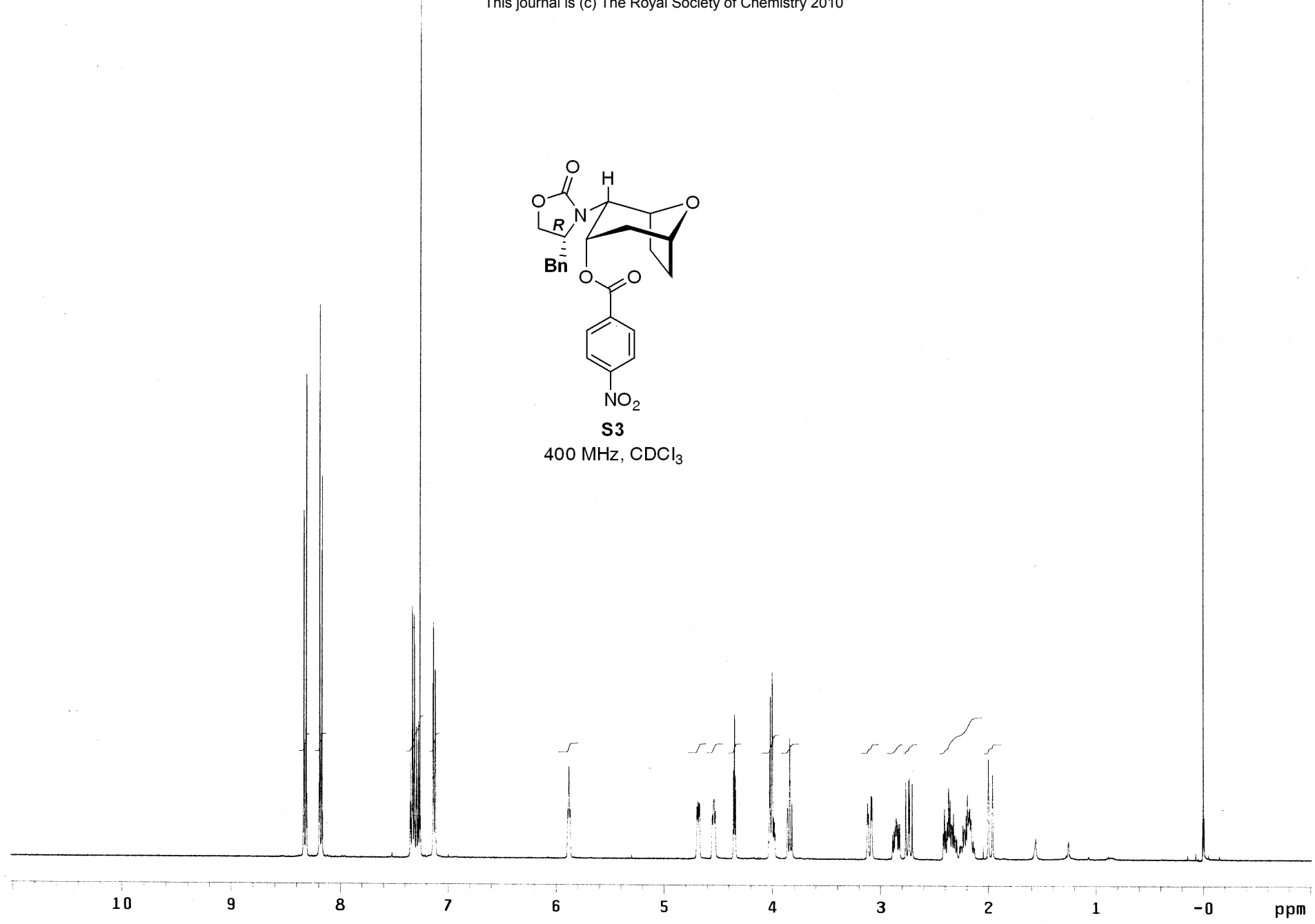
125 MHz, CDCl_3

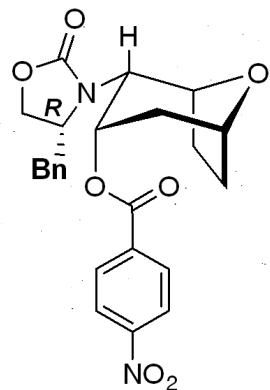




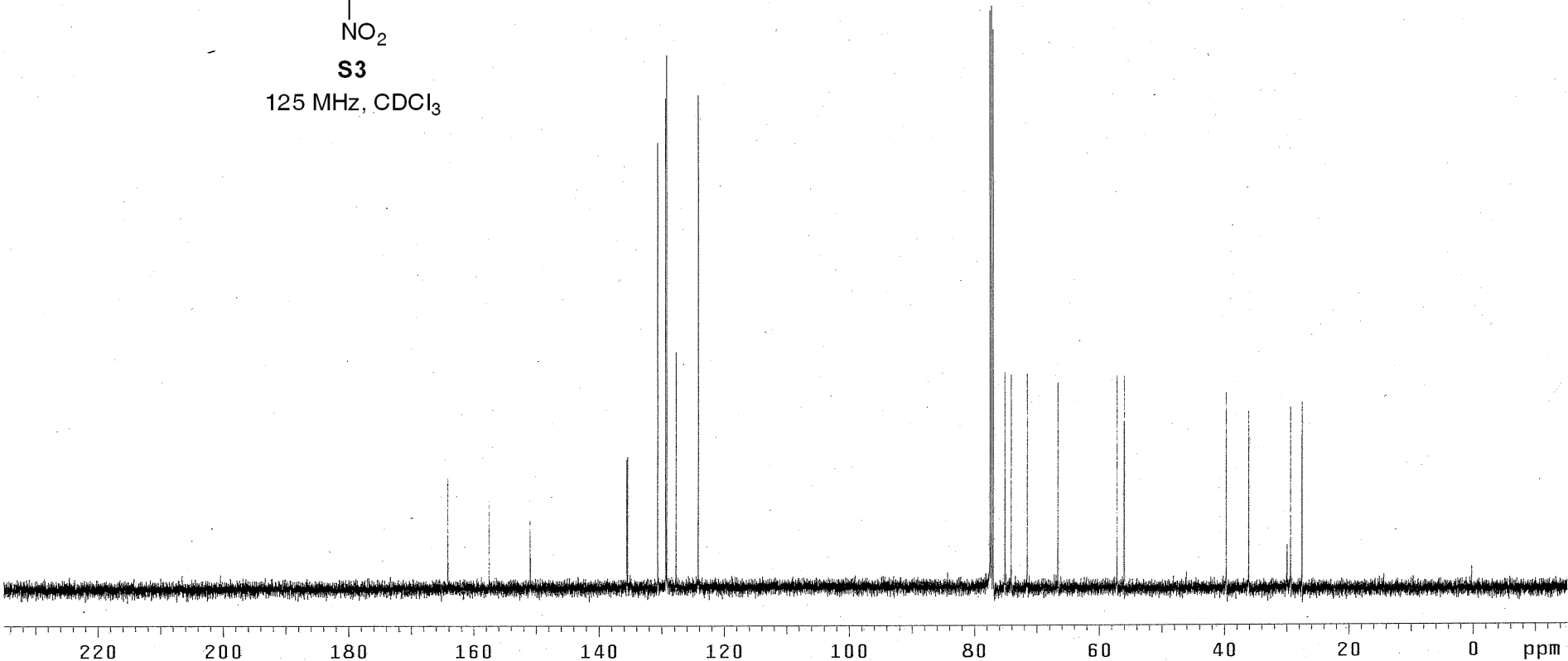
S3

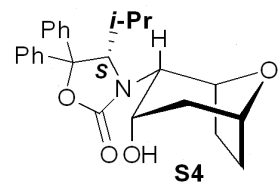
400 MHz, CDCl₃



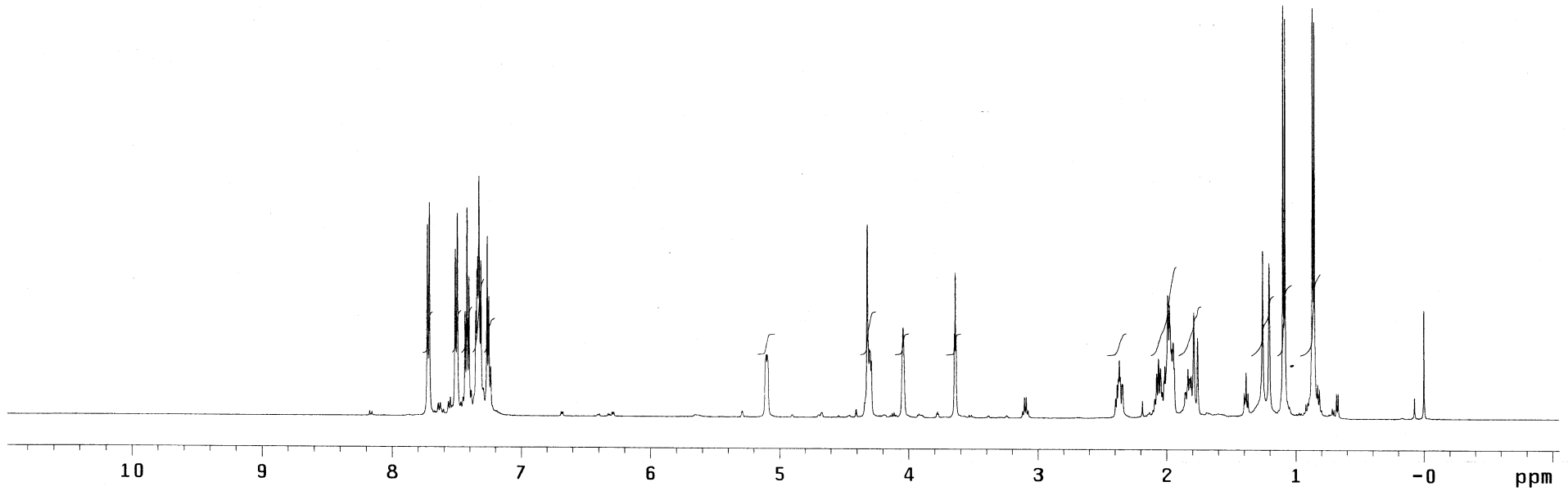


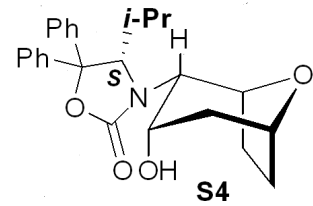
S3
125 MHz, CDCl₃



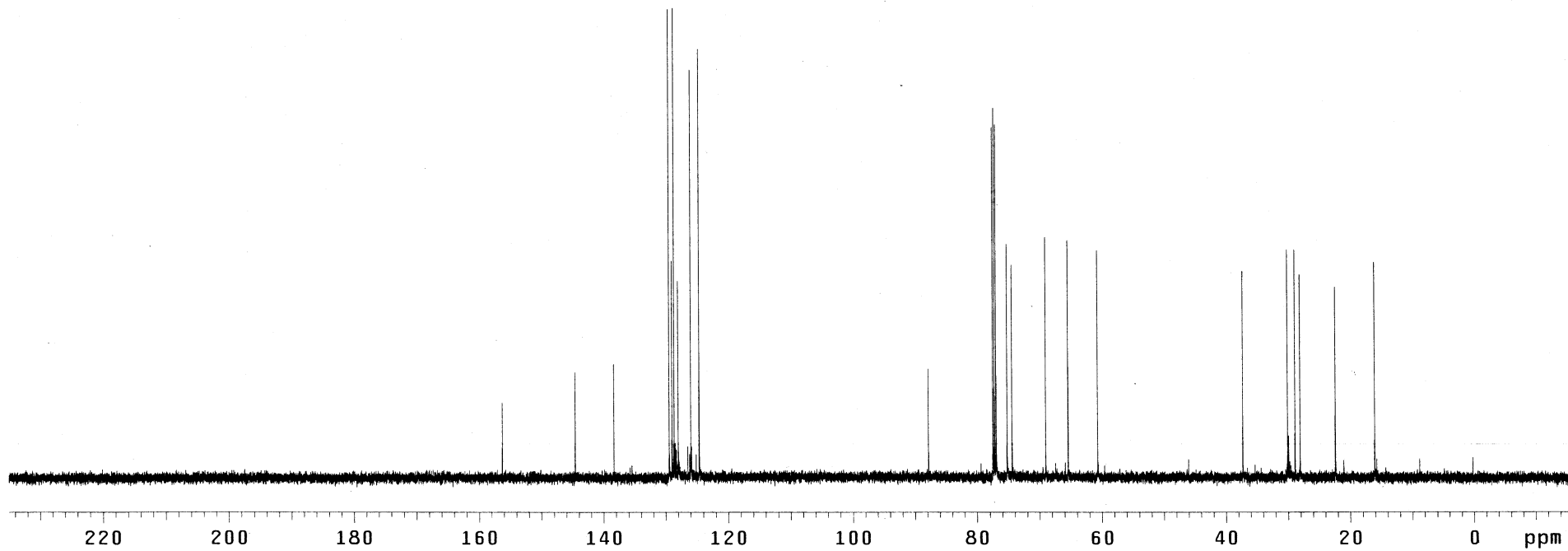


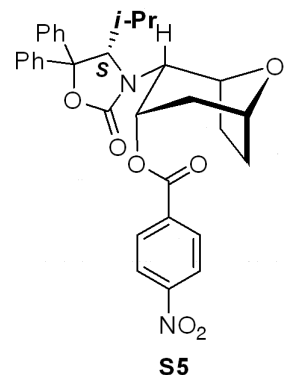
500 MHz, CDCl₃





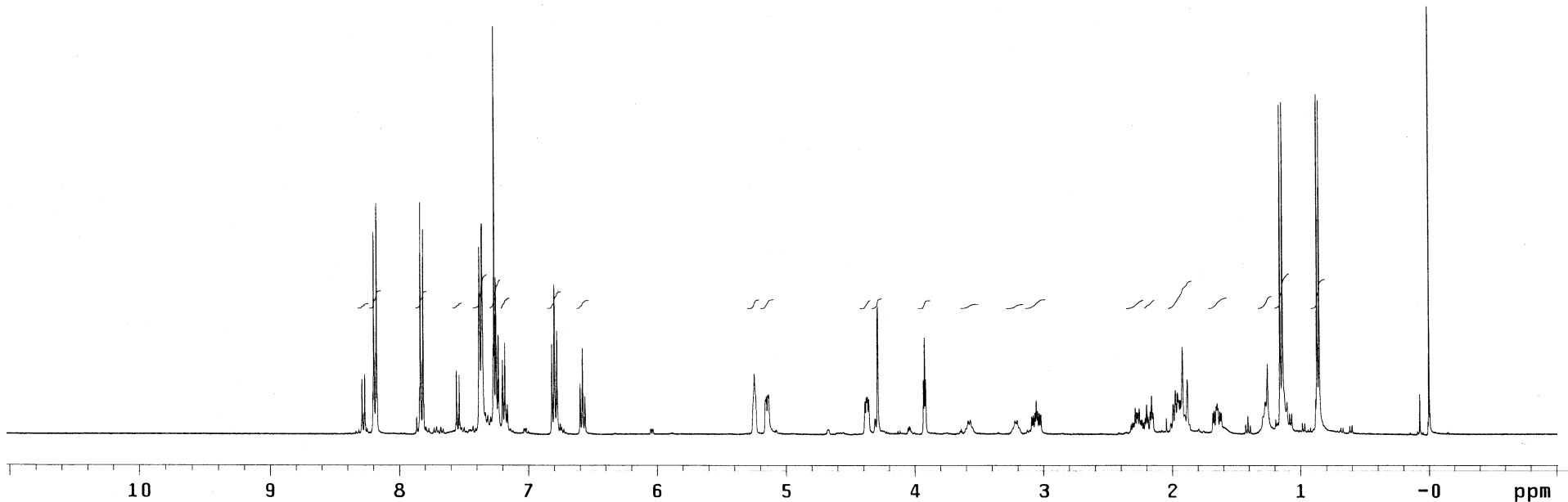
125 MHz, CDCl_3

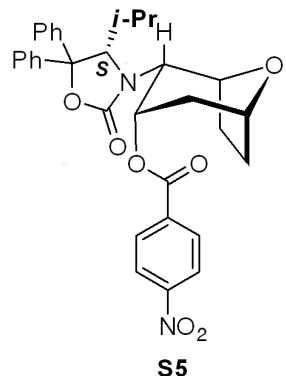




S5

400 MHz, CDCl_3
~4:1 rotamers





100 MHz, CDCl_3

